Water Air Soil Pollut (2015) 226: 278
DOI 10.1007/s11270-015-2546-8

Nitrate Uptake from Water by Means of Tailored Adsorbents

G. V. Nunell · M. E. Fernandez · P. R. Bonelli · A. L. Cukierman

Received: 26 February 2015 / Accepted: 21 July 2015 / Published online: 1 August 2015

Abstract Two different adsorbents directed to nitrate removal from water were developed from *Parkinsonia aculeata* wood. An activated carbon was obtained by chemical activation with K_2CO_3 at 800 °C, whereas another adsorbent was prepared using a dilute solution of NH_4Cl at 450 °C. Elemental compositions, surface functional groups, and textural parameters of both adsorbents were determined and compared with those of a commercial activated carbon used as a reference. Nitrate adsorption assays were carried out to examine the effects of solution pH, adsorbent dosage, contact time, and equilibrium adsorption isotherms. The adsorbent obtained with K_2CO_3 showed a well-developed pore structure (S_{BET}=777 m^2/g; V_T=0.35 cm^3/g) and neutral character, while the one prepared with NH_4Cl exhibited a low porous development (S_{BET}=58 m^2/g; V_T=0.03 cm^3/g), acidic nature, and a noticeably high N content. The latter attained the highest nitrate removal efficiency, with a maximum adsorption capacity (X_{mL}=0.40 mmol/g) higher than those estimated for the former (X_{mL}=0.34 mmol/g) and the commercial sample (X_{mL}=0.23 mmol/g), pointing to a predominant role of the chemical surface characteristics, mainly of N-containing groups and basic functionalities. Accordingly, the adsorbent obtained with NH_4Cl represents a friendly novel material especially suited for nitrate removal.

Keywords Activated carbons · Ammonium chloride · Nitrate removal · Potassium carbonate

G. V. Nunell · M. E. Fernandez · P. R. Bonelli · A. L. Cukierman
Programa de Investigación y Desarrollo de Fuentes Alternativas de Materias Primas y Energía (PINMATE), Departamento de Industrias, Facultad de Ciencias Exactas y Naturales, Universidad de Buenos Aires, Intendente Güiraldes 2620, Ciudad Universitaria C1428BGA Buenos Aires, Argentina

G. V. Nunell · M. E. Fernandez · P. R. Bonelli · A. L. Cukierman
Consejo Nacional de Investigaciones Científicas y Técnicas (CONICET), Av. Rivadavia 1917, C1033AAJ Buenos Aires, Argentina
e-mail: analea@di.fcen.uba.ar

A. L. Cukierman (✉)
Cátedra de Farmacotecnia II, Departamento de Tecnología Farmacéutica, Facultad de Farmacia y Bioquímica, Universidad de Buenos Aires, Junín 956, C1113AAD Buenos Aires, Argentina
e-mail: analea@di.fcen.uba.ar

1 Introduction

Several nitrogen-containing compounds have been found as common pollutants in drinking water and various wastewaters. Nitrate, due to its high water solubility, is possibly the most widespread groundwater contaminant in the world, imposing a serious threat to drinking water supplies including eutrophication and some diseases, such as cyanosis and cancer of the alimentary canal. Therefore, in recent years, much attention has been paid to remove this contaminant from water and several techniques have been applied for this purpose, including biological denitrification, reverse osmosis, electrodialysis, breakpoint chlorination, ion exchange, membrane filtration, and adsorption (Anirudhan and Rauf 2013; Demiral and Gündüzoğlu

2010; Ji et al. 2014; Kilpimaa et al. 2014; Mukherjee and De 2014; Sahinkaya et al. 2014; Wan et al. 2012; Wang et al. 2007). However, current available technologies for NO_3^- removal suffer from low treatment efficiency and high operation cost and generate additional by-products (Bhatnagar and Sillanpää 2011). Adsorption represents an attractive option as it is considered a simple, fast, and inexpensive method. Various adsorbents have been examined for the removal of this priority pollutant from aqueous solution including organoclays and organosilicas (Bagherifam et al. 2014; Seliem et al. 2013), graphene (Ganesan et al. 2013), red mud (Cengeloglu et al. 2006), layered double hydroxides (Islam and Patel 2010), and modified pine sawdust (Keränen et al. 2013). Activated carbons are one of the most studied adsorbents, due to their versatility and wide range of application, although these materials are not very effective for the removal of nitrate ions from water (Mukherjee and De 2014; Loganathan et al. 2013; Cho et al. 2011; Öztürk and Bektas 2004). Since properties of activated carbons depend on the precursor material and the process conditions used for their preparation, it is interesting to develop this kind of adsorbents with improved nitrate adsorption performance, employing low cost, abundant precursors.

P. aculeata is a worldwide invasive arboreal species that is in the league of the most noxious woody plants. It can form dense and often impenetrable thorny thickets along watercourses impeding access to drinking water supplies, excluding native vegetation, and contributing to soil erosion (Cochard and Jackes 2005; Deveze 2004). Several methods have been proposed for the management of this invasive species, but they failed in finding out the eradication (CSIRO 2011). Hence, wood from this species may result an attractive option for its use as a precursor of adsorbent materials, not only due to its abundance and renewable character but also to find out a solution to the existing management problem of this invasive species.

In the present work, we explore the possibility of using *P. aculeata* wood to develop two different adsorbent materials, directed to optimize nitrate removal from water. The adsorbents are prepared by the chemical activation process using solutions of K_2CO_3 and NH_4Cl as chemical reagents and different operational conditions. These reagents represented environmentally friendlier alternatives to the more traditional activating agents, such as H_3PO_4, $ZnCl_2$, and alkali hydroxides, which may generate corrosion, toxicity, and/or disposal problems (Adinata et al. 2007). K_2CO_3, a known food additive, is considered non-toxic, and it is easily removed by water washing (Xiao et al. 2014); likewise, residual NH_4Cl extraction after the carbonization step is not necessary because it sublimates at a moderate temperature (338 °C) (Balci et al. 1994). It should be stressed that the development of adsorbent materials especially suitable for nitrate uptake using the above-mentioned precursor in combination with solutions of K_2CO_3 and NH_4Cl has been almost unexplored. The materials obtained are characterized and tested in the removal of nitrate from model dilute solutions. Adsorption isotherms are obtained and modeled. The maximum adsorption capacities of the adsorbents are discussed in terms of their textural and chemical characteristics and also compared with those determined for a commercial activated carbon.

2 Materials and Methods

2.1 Precursor

P. aculeata debarked trunks were obtained from a rural area located in Buenos Aires province, Argentina. They were air dried, crushed, milled, and sieved to obtain fractions of different particle sizes. The selected fractions were then washed and dried at 60 °C until constant weight was attained.

2.2 Preparation of the Adsorbents

A procedure similar to that reported in our previous work for potassium hydroxide-derived AC (Nunell et al. 2012) was followed for the chemical activation with potassium carbonate. Prior to the activation stage, a sample of 60 g of the precursor of average particle size of 1500 μm was placed inside a horizontal fixed-bed stainless steel tubular reactor placed inside an electric furnace. Thermal treatment of the sample was carried out under flowing air (150 mL/min) at a heating rate of 10 °C/min until 350 °C; this final temperature was maintained for 1 h. The carbonized precursor obtained was impregnated with a K_2CO_3 solution (50 wt%) for K_2CO_3/carbonized precursor mass ratio of 1. The mixture was dried at 80 °C in an oven. The resulting samples were then placed in the same reactor used for the carbonization stage, heated from room temperature to 300 °C at 10 °C/min, and held for 2 h. Subsequently,

the temperature was raised to 800 °C at the same heating rate and held for 2 h before cooling down. The whole activation process was carried out under a nitrogen flow rate of 150 mL/min. The resulting material was washed with 0.1 N HCl acid solution and with distilled water until absence of chloride ions in the washing water. The washed samples were then dried in an oven at 110 °C to constant weight. The activated carbon obtained was designated as PA-K.

On the other hand, a sample of 60 g of the precursor of average particle size of 750 μm was impregnated with a NH_4Cl solution (5 wt%), using NH_4Cl/precursor mass ratio of 0.1. The slurry obtained was then dried in an oven at 110 °C for 2 h. Afterwards, it was thermally treated in the reactor above mentioned at 450 °C for 0.5 h under N_2 flow (150 mL/min). The resulting material was thoroughly washed with distilled water, till an absence of chloride ions in the washing waters was attained. Finally, it was dried at 110 °C to constant weight. The so-obtained sample was designated as PA-N. Yields were estimated from weight differences.

2.3 Characterization

Chemical characteristics of the different materials were determined by elemental analyses using a Carlo Erba EA1108 instrument. Ash contents were determined according to the American Society of Testing and Materials (ASTM) standards with a thermal analyzer TA instrument SDT Q-600.

Contents of the total and individual surface acidic/polar oxygen functional groups (carbonyls, phenols, lactones, and carboxyl groups) for the different adsorbents were determined according to a procedure described in detail elsewhere (Fernandez et al. 2012; Nunell et al. 2012). Briefly, 0.5 g of each sample was mixed with 50 mL of a 0.05 N solution of sodium ethoxide, sodium hydroxide, or sodium bicarbonate in closed flasks and agitated for 24 h at room temperature. Then, the suspensions were filtered and 10 mL aliquot of each resulting filtrate was added to 15 mL of a 0.05 N HCl acid solution. The resulting solutions were back-titrated with 0.05 N NaOH. The total content of basic surface groups was also assessed. Of each sample, 0.5 g was added to 50 mL of 0.05 M HCl acid solutions, and the titration solution employed was 0.05 N NaOH.

The surface functionalities of the developed adsorbents and the commercial sample were complementary identified by Fourier transformed infrared (FTIR) spectroscopy. A Perkin Elmer IR Spectrum BXII spectrometer was used. The spectra were recorded within the range 600–4000 cm^{-1} wave numbers.

Textural properties of the derived adsorbents and the commercial sample were determined from N_2 adsorption–desorption isotherms, using an automatic Micromeritics ASAP-2020 HV volumetric sorption analyzer. Prior to the measurements, each sample was dried in an oven at 110 °C up to constant weight and then outgassed under vacuum at 120 °C overnight. The specific surface area (S_{BET}) was calculated by the Brunauer–Emmett–Teller method. Total pore volumes (V_t) were determined from the amount of nitrogen adsorbed at the highest relative pressure (P/P_0~0.99). The mean pore width (W) was estimated as $W=4V_t/S_{BET}$ (Martín-González et al. 2014). Pore size distributions (PSDs) were calculated from N_2 adsorption data by means of the DFT Plus Software (Micromeritics Instrument Corporation), based on the non-local density functional theory, that assumes slit pore shape.

2.4 Nitrate Adsorption Assays

Nitrate removal effectiveness for the different adsorbents was examined from batch assays using model dilute solutions. Analytical grade sodium nitrate and distilled water were employed to prepare a nitrate ion stock solution (16 mmol/L). It was further diluted as required to obtain model solutions (0.1–6 mmol/L). Nitrate ion concentrations in solution were determined employing an UV-visible spectrophotometer (Shimadzu UVmini-1240) at 201 nm. Slurries were prepared in glass flasks by contacting model solutions with samples of the adsorbent of 375 μm average particle size. The flasks were then placed in a shaker. All the assays were conducted at temperature of 25±1 °C and at constant speed of 300 rpm. For all the systems studied, equilibrium conditions were completely verified.

The effect of the solution's pH on the equilibrium adsorption of nitrate ions was examined. For these experiments, 0.5 g of each adsorbent were contacted with 50 mL of 1.61 mmol/L nitrate solutions, and the pH of the system was adjusted to values between 2 and 12. Values of the pH were kept constant during the tests, with variations within ±0.2 U. Once equilibrium was attained, the slurries were filtered through 0.45-μm membranes, and nitrate

concentrations in solution were determined as described above. Nitrate removal percentages were calculated as follows:

$$\text{Removal}\ (\%) = \left[(C_0 - C_e)\Big/C_0\right] \times\ 100 \qquad (1)$$

where C_0 and C_e are the initial and equilibrium nitrate concentrations in solution, respectively. The optimum pH value determined from these assays was selected for the other adsorption experiments.

The influence of the sample's dose on the adsorption of nitrate ions was examined. For that purpose, different weighed amounts (0.05–1.5 g) of each adsorbent were contacted with 50 mL of 1.61 mmol/L nitrate solutions. The amount of nitrate removed was determined as indicated above.

Kinetic experiments were performed agitating 0.5 g of each adsorbent with 50 mL of 1.6 mmol/L nitrate solutions. Samples were withdrawn at different times, and nitrate removal was determined as already described. Preliminary experiments were conducted in order to investigate possible external and intraparticle mass transfer resistances.

Nitrate adsorption isotherms onto the developed adsorbents and the commercial activated carbon were obtained by mixing 50 mL of the nitrate solutions of different concentrations (0.1–6 mmol/L) with 0.5 g of each adsorbent in closed Erlenmeyer flasks. The suspensions were shaken at 25 °C, until equilibrium was reached. The amount of nitrate adsorbed at equilibrium per mass of sample, q_e (mmol/g), was calculated as follows:

$$q_e = (C_0 - C_e)\Big/D \qquad (2)$$

where D is the dose of sample used (g/mL). Duplicate experiments were performed in all the cases, and differences between replicates were less than 2 %. Average values are reported. Solute and adsorbent blanks were simultaneously run for control under corresponding conditions.

3 Results and Discussion

3.1 Chemical Characterization

Table 1 reports chemical characteristics of *P. aculeata* wood, the prepared adsorbents, and the commercial sample used as a reference as well as yields for the developed adsorbents. The results indicate that the treatments applied led to noticeable modifications in the raw material. Both adsorbents present higher contents of ash, C, and N, but less contents of H and O than the precursor. The activated carbon developed with potassium carbonate, PA-K, shows an elemental composition similar to that of the commercial sample used for comparison, whereas PA-N presents a less C content but noticeable higher contents of N, H, and O. The higher O and H contents could be attributed to the lower temperature applied for PA-N preparation likely preventing thermal decomposition of some oxygen functional groups. In turn, the increase in N might be due to the incorporation of some N functionalities from the NH_4Cl used as chemical agent for its development. Similar contents of N were also obtained by Balci et al. (1994) who reported that most of the nitrogen from NH_4Cl remained in the solid matrix at 450 °C, whereas this reactant, as such, is mainly decomposed at that temperature. As previously observed by our team (Nunell et al. 2012), enrichment in N contents in the adsorbent enhances nitrate adsorption, a desirable feature. Besides, PA-N preparation led to a markedly

Table 1 Yield and chemical characteristics of *Parkinsonia aculeata* wood (PA), the adsorbent prepared with NH_4Cl (PA-N), the activated carbon developed with potassium carbonate (PA-K), and the commercial sample (CAC)

Sample	Ash wt% (dry basis)	Elemental analysis wt% (dry and ash free basis)				pH	Yield (%)
		C	H	N	O*		
PA	1.4	48.0	5.7	0.2	46.1	–	–
PA-N	2.4	65.4	3.1	6.3	25.2	4.1	45.5
PA-K	3.1	80.6	1.6	0.4	17.4	7.2	21.3
CAC	5.8	86.3	2.1	0.6	11.0	3.0	–

*Estimated by difference

higher yield than that attained for PA-K (45.5 and 21.3 %, respectively), probably also due to the moderate temperature and operating conditions used for the preparation of the former and to the fact that NH_4Cl may favor dehydration over depolymerization during the pyrolysis of the precursor, which frequently increases yields at low temperatures (Huidobro et al. 2001). Studying the effect of the impregnation with NH_4Cl by thermogravimetric analysis (data not shown), it was seen that degradation of the untreated precursor started around 250 °C and reached a residual weight fraction of 0.26 at 450 °C. Conversely, the NH_4Cl-impregnated precursor started to decompose at lower temperature (180 °C) but reached a higher residual weight fraction of 0.45 at 450 °C (Nunell 2013). According to Balci et al. (1994), NH_4Cl crystallizes in the precursor during the drying step and, in turn, acts as a support during carbonization at temperatures below its decomposition temperature. In the case of PA-K, there was a major release of volatile products at the carbonization temperature, as a result of intensified dehydration and elimination reaction and the gasification of the char (Adinata et al. 2007). PA-N and the commercial sample are acidic, whereas the activated carbon obtained with potassium carbonate has a neutral pH (Table 1).

Contents of the total and individual surface acidic-polar oxygen functional groups as well as total basic functionalities of the developed adsorbents and the commercial sample are presented in Table 2. As observed, the development of these functionalities on the surface of the adsorbents markedly depends on the reagent used and treatment conditions applied for their preparation. PA-N and CAC possess higher contents of acidic oxygen functional groups than PA-K. This is in accordance with the more acidic pH of these samples (Table 1), likely due to the chemical agent and lower temperature involved in their preparation that could prevent thermal decomposition of some acidic oxygen functionalities. Among surface acidic functionalities, all the investigated adsorbents present major contribution of phenols and lactones. PA-N is characterized by the lack of carbonyl groups, whereas PA-K possesses the highest content of carbonyls. The lower content of carboxyl groups evidenced for PA-K could be attributed to their thermal decomposition at the higher temperature applied for its development. In turn, the commercial activated carbon shows lack of basic functionalities, whereas PA-N has an intermediate content, and PA-K presents the highest one, in accordance with the basic nature of the activating reagent used in its development. Moreover, Lorenc-Grabowska et al. (2010) also reported that the carbonization of the precursor prior to the chemical activation leads to intensify the development of basic functionalities in the resulting activated carbon.

Table 2 Total and individual quantities of acidic surface functional groups and basic functionalities determined for the adsorbent prepared with NH_4Cl (PA-N), the activated carbon developed with potassium carbonate (PA-K), and the commercial sample (CAC)

	PA-N (meq/g)	PA-K	CAC
Total acidic oxygen functional groups	2.3	1.3	2.0
Phenols and lactones	1.7	0.7	1.0
Carboxyls	0.6	0.1	0.7
Carbonyls	–	0.5	0.3
Basic functionalities	0.3	0.9	–

The FTIR spectra of the precursor, the derived adsorbents, and the commercial sample are shown in Fig. 1. For all the samples, an absorption band may be observed at wave numbers between 3200 and 3600 cm^{-1} which is representative of hydroxyl functional groups on the surface of the different materials. This broad band is also related to hydrogen bonding and suggests that water still remained in the samples (Apaydın-Varol and Pütün 2012; Martín-González et al. 2014). For PA-N spectra, this broad band has a maximum intensity at 3400 cm^{-1} and a shoulder at 3200 cm^{-1}. Such a peak bifurcation is often observed in compounds that have primary amines in their chemical structure (Kante et al. 2012). Because of the higher nitrogen content of PA-N, bands attributed to C–N stretching vibrations overlap with C–C absorption bands resulting in a stronger and broad peak at ~1600 cm^{-1}. A small band around this position, frequently associated with the presence of aromatic rings, is barely perceived in the rest of the adsorbent spectra. Absorption peaks at wave numbers between 2440 and 2350 cm^{-1} are observed in every spectra and may be attributed to C–O asymmetric stretching vibration of CO_2. For PA and PA-K, absorption bands are observed at wave numbers between 2950 and 2800 cm^{-1}; these bands are assigned to C–H stretching modes of methyl and methylene groups present in aliphatics, olefinics, and aromatics. In the PA spectra, an absorption band between 1750 and 1600 cm^{-1} is

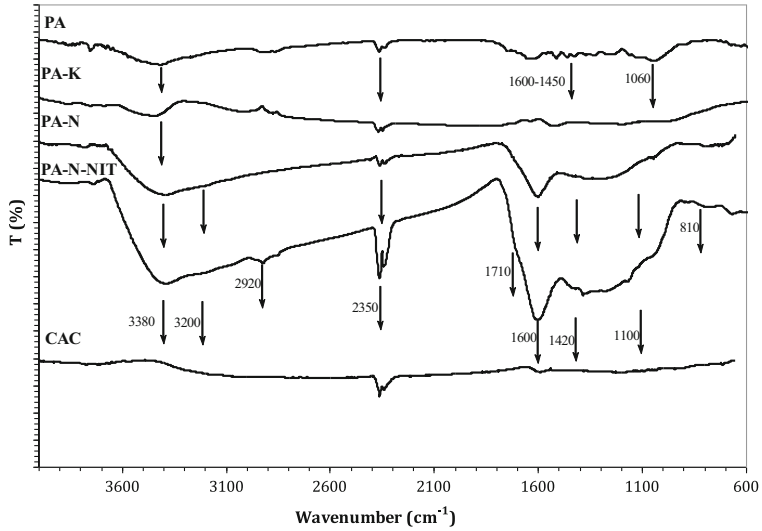

Fig. 1 FTIR spectra for the precursor (PA), the activated carbon developed with potassium carbonate (PA-K), the commercial sample (CAC), the adsorbent prepared with NH_4Cl (PA-N) and further loaded with nitrate ion (PA-N-NIT)

observed. This band is assigned to C=O present in carbonyls, ketones, aldehydes, or ester groups and to C=C present in olefinic vibrations in aromatic region (Popescu et al. 2013). The aromatic structure is also confirmed in this sample by the strong absorption band visualized at around 1060 cm^{-1} that indicates the presence of lignin. The aromatic skeletal C=C vibration absorptions occur in the 1600–1450 cm^{-1} region. The relative intensity of such bands varies frequently when electronegative substituents are found in the aromatic rings because of their disturbing effect on the electron density distribution (Fu et al. 2009). Furthermore, a strong absorption band at wave numbers from 1420 to 1100 cm^{-1} is observed in the FTIR spectra of PA-N, demonstrating that oxygen is functioning to stretch carboxylic groups and that carboxylate groups are present on the surface of this adsorbent material (Moussavi et al. 2013). These adsorbents were also examined by FTIR spectroscopy after the nitrate adsorption experiments. However, only the spectrum obtained for the nitrate-loaded PA-N (PA-N-NIT) differ from the original sample. This spectrum is also presented in Fig. 1. It may be observed the presence of characteristic bands of ionic nitrate at 1420–1330 and 850–790 cm^{-1}; also, the bands corresponding to alkyl-carbonyl groups with nitrile type substituent (2985–2895, 2300–2085, 1770–1700, 1470–1400 cm^{-1}) appear in the spectrum of PA-N-NIT, suggesting the formation of a chelate complex of nitrate anion with the N-containing groups, such as amidine and/or amino groups that might be incorporated with the NH_4Cl treatment.

3.2 Textural Characterization

N_2 adsorption–desorption isotherms for the developed adsorbents and the commercial activated carbon are illustrated in Fig. 2. Noticeable similitude for the shapes of the N_2 adsorption isotherms of PA-N and PA-K may be observed. The adsorption branch of the isotherms resembles that of a type I isotherm in the IUPAC classification, showing high adsorption at low relative pressure, characteristics of microporous materials. Nevertheless, the presence of a hysteresis loop in both isotherms, being a little more pronounced for PA-N, reveals the existence of mesopores. The shape of these loops is similar to those of type H4, often associated with narrow slit-like pores (Sangwichien et al. 2002). The isotherm for CAC is quite similar to type IV of the IUPAC classification, suggesting a surface structure with mesopore predominance. According to this classification, the hysteresis loop observed at the commercial sample corresponds to H3 and H4 types, respectively, indicating the presence of slit-shaped pores. Moreover, there are remarkable differences in N_2 adsorption capacity for the different adsorbents studied. The commercial sample adsorbs a larger volume of nitrogen than the developed adsorbents, pointing to a more pronounced pore structure development. The low nitrogen volume adsorbed at P/P_0~1 for PA-N indicates that this sample has a poorly developed porous structure. The porous

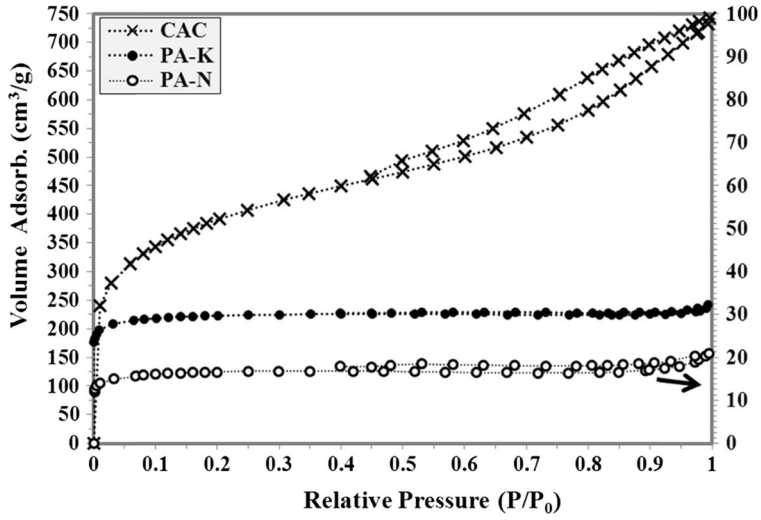

Fig. 2 N_2 adsorption–desorption isotherms for the adsorbent prepared with NH_4Cl (PA-N), the activated carbon developed with potassium carbonate (PA-K), and the commercial sample (CAC)

structure parameters calculated from the nitrogen adsorption–desorption isotherms are summarized in Table 3. It can be observed that PA-N has the lowest BET surface area (58 m^2/g) and a similar contribution of micropores and mesopores, whereas PA-K possesses a more pronounced pore structure development (777 m^2/g) and a major contribution of micropores to the total pore volume. Adinata et al. (2007) found that specific surface area and micropore volume increased up to a temperature of 800 °C (the same used for PA-K). It was suggested that this was related to the presence of K_2CO_3 in the interior of the precursor which restricted the formation of tar and other liquids and inhibited the shrinkage of the precursor particle and also that, in inert atmosphere, carbon partially reduced the impregnated K_2CO_3, consumed through the formation of CO. CAC has the highest value of BET surface area (1424 m^2/g) and a predominantly mesoporous structure.

Table 3 Textural characteristics of the adsorbent prepared with NH_4Cl (PA-N), the activated carbon developed with potassium carbonate (PA-K), and the commercial sample (CAC)

	PA-N	PA-K	CAC
S_{BET} (m^2/g)	58	777	1424
Total pore volume (cm^3/g)	0.03	0.35	1.08
Micropore volume[a] (%)	49.6	60.0	26.3
Mesopore volume[b] (%)	50.4	40.0	73.7
Mean pore width (nm)	1.91	1.81	3.04

[a] Determined by the DFT method

[b] Estimated by difference

3.3 Nitrate Adsorption

3.3.1 Effect of the Solution pH

The influence of the solution pH on nitrate removal, at equilibrium, for the prepared adsorbents and the commercial sample is displayed in Fig. 3. As seen, the removal of nitrate ions strongly depends on the solution pH in all cases. Acidic pHs favor nitrate adsorption onto the different materials, whereas the removal levels decrease with increasing pH and are almost negligible above pH 7 (data not shown). This trend is more pronounced for PA-N sample. Since this sample has a

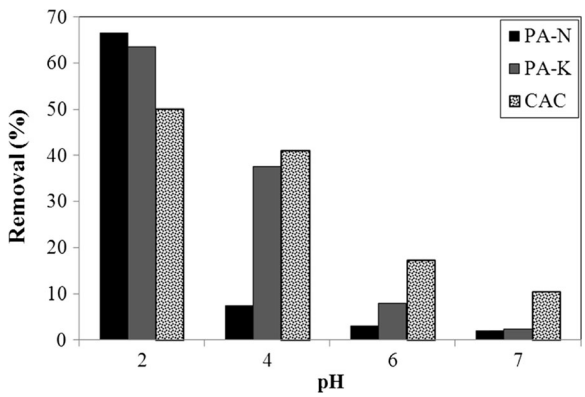

Fig. 3 Effect of the solution pH on the removal of nitrate ions for the adsorbent prepared with NH_4Cl (PA-N), the activated carbon developed with potassium carbonate (PA-K), and the commercial sample (CAC)

poorly developed porous structure, the removal of nitrate ions could be mainly attributed to interactions between the adsorbate and the functional groups present on its surface. The degree of protonation of the surface functional groups is reportedly known to depend on the solution pH. At acidic pH, a major fraction of the negative sites on the adsorbent should be occupied by H^+ ions via electrostatic attraction producing protonated surface functional groups, which provide electrostatic attraction forces for nitrate anions. With increasing pH, the surface of the adsorbent should become more negatively charged and a higher concentration of hydroxyl groups should be present in the solution, thus leading to reduce the levels of nitrate adsorption. For PA-K and CAC samples, the adsorption decreases more gradually as the pH increases, likely because these adsorbents have a more pronounced porous structure providing more adsorption sites.

3.3.2 Effect of the Sample Dose

The effect of the adsorbent dosage on nitrate removal percentages, at equilibrium conditions, is illustrated in Fig. 4. The results in the figure show a pronounced increase of nitrate removal percentages with increasing doses up to 0.5 g/50 mL for the developed adsorbents and up to 1 g/50 mL for the commercial sample. The increase in the removal percentage with increasing doses is probably due to the greater adsorbent surface area and pore volume available, the higher adsorbent dose providing more functional groups and active adsorption sites. In turn, the almost negligible change in the nitrate removal percentage for doses above 1 g/50 mL may be attributed to an excess of available active sites for the investigated conditions.

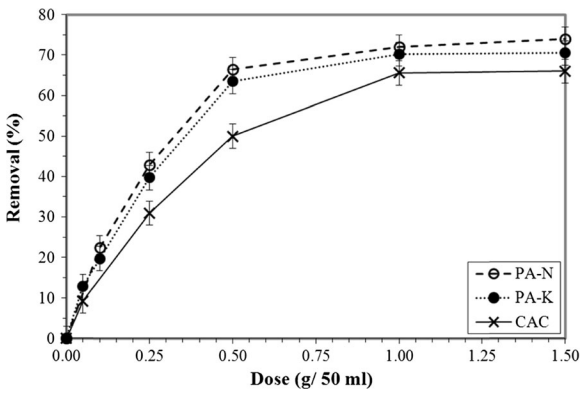

Fig. 4 Effect of the sample dose on the removal of nitrate ions for the adsorbent prepared with NH_4Cl (PA-N), the activated carbon developed with potassium carbonate (PA-K), and the commercial sample (CAC)

It should also be mentioned that the minimum amount of adsorbent corresponding to the highest nitrate uptake was taken as the optimum adsorbent dose. Since a small increment in nitrate uptake for CAC was observed by duplicating the dose from 0.5 to 1 g/50 mL, the value of 0.5 g/50 mL was considered as the best adsorbent doses for every system studied and used for the subsequent experiments.

3.3.3 Kinetic Results

Kinetic experimental data obtained for nitrate adsorption onto the developed adsorbents and the commercial sample were fitted to a pseudo-second-order rate model, which has been widely employed to describe adsorption kinetics (Ho 2006). This model correlates well kinetic data in systems in which chemisorption involving valence forces through the sharing or exchange of electrons between the adsorbent and the adsorbate constitutes the rate-limiting step. The model was applied in the non-linear form because of the better ability to predict kinetic parameters (Martín-González et al. 2014). Its mathematical expression is given by

$$q_t = \left(q_{eH}^2 K_H t\right) \Big/ \left(1 + q_{eH} K_H t\right) \quad (3)$$

q_t in Eq. (3) represents the amount of nitrate adsorbed at any time t (mmol/g), K_H, the adsorption rate constant (g/mmol min), and q_{eH}, the amount of nitrate adsorbed at equilibrium per unit mass of sample (mmol/g).

Kinetic data for nitrate adsorption onto the different adsorbents and model predictions are illustrated in Fig. 5. As seen, the removal rates at the initial stages of the adsorption are very fast for all the samples and slow gradually down as equilibrium is attained. The fast adsorption at the initial stage may be due to the higher driving force making fast transfer of adsorbate ions to the surface of the adsorbent particles and the availability of remaining active sites on the adsorbent surface. The decreased removal rates indicate a possible monolayer formation of nitrate ions on the outer surface. Nitrate adsorption reaches equilibrium in about 10, 30, and 300 min for CAC, PA-N, and PA-K, respectively. The results are in line with the more pronounced mesoporous structures of CAC and likely with the easy accessibility of nitrate ions to active sites present on PA-N surface due to its low-developed porous structure. In opposition,

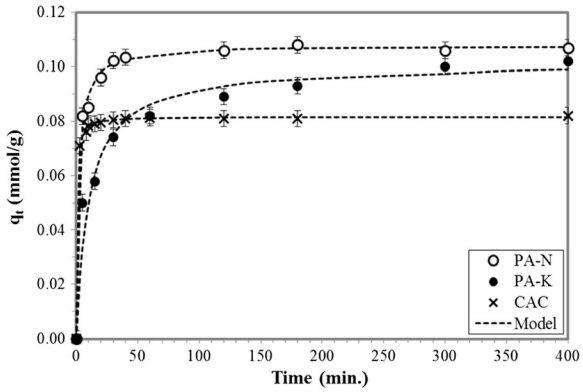

Fig. 5 Kinetics of nitrate ion adsorption onto the adsorbent prepared with NH_4Cl (PA-N), the activated carbon developed with potassium carbonate (PA-K), and the commercial sample (CAC). Comparison between the experimental data and the pseudo-second-order model predictions

the predominance of microporous structures of PA-K seems to impede a rapid interaction of the adsorbate with the adsorbent active sites. The representation of adsorption kinetic results by the pseudo-second-order kinetic model agrees well with the experimental data, in all the cases. Table 4 summarizes the model parameters for nitrate adsorption which were also estimated by non-linear regression analysis for a 5 % significance level, by minimizing the following objective function (OF):

$$\mathrm{OF} = \sum_{i=1}^{N} \left(q_{\mathrm{exp}} - q_{\mathrm{mod}}\right)^2 \tag{4}$$

As may be observed in Fig. 5, the kinetic model applied describes properly the experimental data (Table 4). The rate constant estimated for nitrate adsorption onto the commercial activated carbon sample is markedly superior to those estimated for the adsorbents, whereas the q_{eH} value is rather lower than those obtained for the developed adsorbents.

Table 4 Estimated parameters of the pseudo-second-order kinetic model for nitrate adsorption onto the adsorbent prepared with NH_4Cl (PA-N), the activated carbon developed with potassium carbonate (PA-K), and the commercial sample (CAC)

	q_{eH} (mmol/g)	K_H (g/mmol min)	R^2
PA-N	0.108	4.5	0.991
PA-K	0.101	1.0	0.986
CAC	0.081	26.7	0.980

3.3.4 Nitrate Adsorption Isotherms

Two-parameter Langmuir and Freundlich models were applied to represent the experimental nitrate adsorption isotherms. The Langmuir model proposes that adsorption onto a homogeneous surface occurs by formation of a monolayer, without interaction between adsorbed molecules, and is represented by the following equation:

$$q_e = \left(K_L X_{mL} C_e\right) \Big/ \left(1 + K_L C_e\right) \tag{5}$$

where X_{mL} (mmol/g) and K_L (L/mmol) are Langmuir constants related to adsorption capacity and energy of adsorption, respectively. The dimensionless constant separation factor (R_L) was also estimated according to Ganesan et al. (2013):

$$R_L = 1 \Big/ \left(1 + K_L C_0\right) \tag{6}$$

R_L values indicate the type of isotherm to be irreversible (R_L=0), favorable (0<R_L<1), linear (R_L=1), or unfavorable (R_L>1). The Freundlich model assumes that adsorption onto a heterogeneous surface occurs with interaction between adsorbed molecules. The equation representing this model is (Singh et al. 2012):

$$q_e = K_F (C_e)^{n_F} \tag{7}$$

where K_F and n_F are Freundlich constants; n_F gives an indication of how favorable the adsorption is, and K_F (mmol/g (L/mmol)^{nF}), of the adsorption capacity of the adsorbent.

Additionally, three-parameter Khan and Radke–Prausnitz models (McKay et al. 2014) were also applied, covering both extremes, Langmuir on one and Freundlich on the other extreme. These models are represented by the Eqs. (8) and (9), respectively, as follows:

$$q_e = \left(K_K X_{mK} C_e\right) \Big/ \left(1 + K_K C_e\right)^a \tag{8}$$

$$q_e = \left(K_{RP} X_{mRP} C_e\right) \Big/ \left(1 + K_{RP} C_e^{\,b}\right) \tag{9}$$

where X_{mK} and X_{mRP} (mmol/g) are constants related to adsorption capacity; K_K and K_{RP} (L/mmol) are equilibrium constants, and a and b are dimensionless

exponents. All model characteristic parameters were estimated by non-linear regression analysis by minimizing the objective function described earlier (Eq. 4). The appropriateness of the models to represent the experimental data was examined from the standard deviation (s), which was estimated according to

$$s = 100 \times \left[\sum_{i=1}^{N} \left(q_{ei,\exp} - q_{ei,est}\right)^2 \Big/ (N-P)\right]^{1/2} \quad (10)$$

Nitrate adsorption isotherms at equilibrium, as well as model predictions are shown in Fig. 6a, b. It could be inferred that the adsorbents prepared in the present work, PA-N and PA-K, showed better adsorption performances than the commercial activated carbon sample.

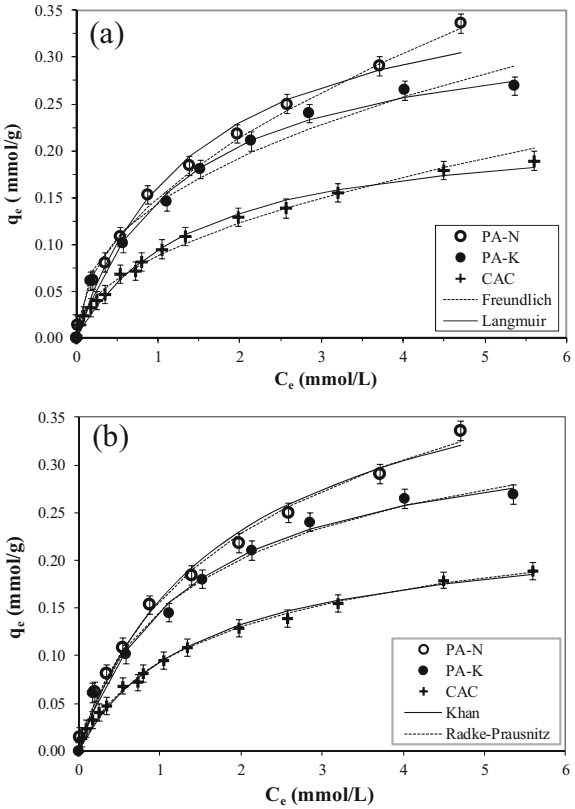

Fig. 6 Nitrate adsorption isotherms for the adsorbent prepared with NH_4Cl (PA-N), the activated carbon developed with potassium carbonate (PA-K), and the commercial sample (CAC). Conditions: D=0.5 g/50 mL, T=25 °C, 300 rpm, pH=2, C_0=0.1–6 mmol/L. **a** Comparison between experimental data and Langmuir and Freundlich model predictions. **b** Comparison between experimental data and Khan and Radke–Prausnitz model predictions

Experimental data was properly described by the two-parameter models (Fig. 6a) and slightly better by the three-parameter models (Fig. 6b). The information obtained from fitting the experimental data to these models is summarized in Table 5. For the two-parameter models, values in this table (s, R^2) indicate that the experimental isotherms obtained for the adsorbent prepared with NH_4Cl and for the commercial sample are best represented by the Freundlich model, suggesting that those adsorbents could exhibit heterogeneous surfaces onto which multilayer adsorption of nitrate could take place. In the case of the activated carbon developed with K_2CO_3, the Langmuir model provides a rather better fit, as evidenced by the higher R^2. This suggests that PA-K has a homogeneous surface where the adsorption of nitrate ions could occur through the formation of a monolayer. In all the cases, the R_L values (Eq. 6) are in the range from 0 to 1 (data not shown), and the n_F values are comprised between 0.42 and 0.51, thus indicating that a favorable adsorption of nitrate ions takes place onto the studied materials. For the three-parameter models, residual sum of squares and

Table 5 Estimated model parameters for nitrate adsorption onto the adsorbent prepared with NH_4Cl (PA-N), the activated carbon developed with potassium carbonate (PA-K), and the commercial sample (CAC)

		PA-N	PA-K	CAC
Langmuir	X_{mL} (mmol/g)	0.40	0.34	0.23
	K_L (L/mmol)	0.68	0.74	0.64
	s (%)	1.3	1	0.7
	R^2	0.983	0.984	0.990
Freundlich	n_F	0.51	0.42	0.49
	K_F [(mmol/g) $(L/mmol)^{nF}$]	0.15	0.14	0.08
	s (%)	0.7	1.4	0.6
	R^2	0.996	0.971	0.991
Khan	X_K (mmol/g)	0.35	0.30	0.20
	K_K (L/mmol)	0.74	0.89	0.81
	a	0.89	0.94	0.93
	s (%)	1.2	0.99	0.59
	R^2	0.990	0.984	0.994
Radke–Prausnitz	X_{RP} [(mmol/g) $(mmol/L)^{b-1}$]	0.32	0.26	0.18
	K_{RP} $(mmol/L)^{-b}$	0.97	1.31	1.069
	b	0.83	0.86	0.86
	s (%)	0.95	1.12	0.46
	R^2	0.994	0.985	0.994

standard deviations were similar to those of the two-parameter models. Predicted maximum adsorption capacities (X_K and X_{RP}) by Khan and Radke–Prausnitz models were more similar to those predicted by the Langmuir model. Values of the exponents of both models >0.8 suggest that the isotherms may approach more to a Langmuir type isotherm, especially for PA-K and CAC.

For the sake of comparison, the maximum adsorption capacities of the different adsorbents were evaluated according to the Langmuir model. X_{mL} value for PA-N (0.40 mmol/g) nearly duplicates that of the commercial sample (0.23 mmol/g), whereas the value estimated for PA-K was intermediate (0.34 mmol/g). The fact that PA-N has a scarcely developed porous structure (58 m^2/g) and the highest nitrate removal capacity, while the commercial sample possesses the highest surface area and the lowest nitrate removal capacity (Tables 3 and 5) reveal that textural characteristics of the samples do not play a key role on nitrate adsorption performance. Accordingly, chemical characteristics of the adsorbent material used might be predominantly related to the removal efficiency of this priority pollutant from aqueous media. In fact, N content of the samples and basic functionalities present on adsorbent surfaces should contribute on nitrate ion uptake. Present results are in accordance with other findings suggesting that protonated amino groups and oxygen basic functionalities, such as pyrones and cromenes, could contribute to an enhanced development of the surface positive charge on the surface of the adsorbent, which should facilitate the uptake of nitrate ions (Keränen et al. 2013; Nunell et al. 2012). Moreover, the X_{mL} values obtained in this work are higher than those previously reported in the literature for the adsorption of nitrate onto different activated carbons (Bhatnagar et al. 2008; Demiral and Gündüzoğlu 2010; Mahmudov and Huang 2011; Nunell et al. 2012; Ota et al. 2013).

4 Conclusion

P. aculeata wood sawdust was successfully converted into two adsorbents of different characteristics, namely a microporous activated carbon of well-developed porous structure (S_{BET}=777 m^2/g; V_T=0.35 cm^3/g) and neutral character (pH~7), and other acidic adsorbent (pH~4) with a scarcely developed porous structure (S_{BET}= 58 m^2/g; V_T=0.03 cm^3/g), but enriched in N surface functionalities. As judged from representing the experimental adsorption isotherms by the Langmuir model, both adsorbents may be considered as potentially suitable for nitrate removal from water, attaining maximum adsorption capacities of 0.34 and 0.40 mmol/g. These values were even higher than the ones previously reported in the open literature for other activated carbons. In particular, the adsorbent developed with NH_4Cl represents a very attractive option due to the simplicity of the preparation process and the moderate operating conditions used, along with the low cost and environmentally friendly nature of the chemical reagent involved.

Acknowledgments The authors gratefully acknowledge Consejo Nacional de Investigaciones Científicas y Técnicas (CONICET), Universidad de Buenos Aires (UBACYT), and Agencia Nacional de Promoción Científica y Tecnológica (ANPCyT-FONCyT) from Argentina, for financial support.

Compliance with Ethical Standards This study was funded by PIP 0183 (CONICET), UBACYT 2104–2017 20020130100605BA (Universidad de Buenos Aires) and PICT 2012–2188 (ANPCYT-FONCYT). The authors declare that they have no conflict of interest. No human participants and/or animals were involved in this research; therefore, no informed consent was required.

References

Adinata, D., Wan Daud, W. M. A., & Aroua, M. K. (2007). Preparation and characterization of activated carbon from palm shell by chemical activation with K_2CO_3. *Bioresource Technology, 98*, 145–149.

Anirudhan, T. S., & Rauf, T. A. (2013). Adsorption performance of amine functionalized cellulose grafted epichlorohydrin for the removal of nitrate from aqueous solutions. *Journal of Industrial and Engineering Chemistry, 19*, 1659–1667.

Apaydın-Varol, E., & Pütün, E. (2012). Preparation and characterization of pyrolytic chars from different biomass samples. *Journal of Analytical and Applied Pyrolysis, 98*, 29–36.

Bagherifam, S., Komarneni, S., Lakzian, A., Fotovat, A., Khorasani, R., Huang, W., Ma, J., Hong, S., Cannon, F. S., & Wang, Y. (2014). Highly selective removal of nitrate and perchlorate by organoclay. *Applied Clay Science, 95*, 126–132.

Balci, S., Dou, T., & Yücel, H. (1994). Characterization of activated carbon produced from almond shell and hazelnut shell. *Journal of Chemical Techology and Biotechnology, 60*, 419–426.

Bhatnagar, A., & Sillanpää, M. (2011). A review of emerging adsorbents for nitrate removal from water. *Chemical Engineering Journal, 168*, 493–504.

Bhatnagar, A., Ji, M., Choi, Y., Jung, W., Lee, S., Kim, S., Lee, G., Suk, H., Kim, H., Mine, B., Kim, S., Jeon, B., & Kang, J. (2008). Removal of nitrate from water by adsorption onto zinc chloride treated activated carbon. *Separation Science and Technology, 43*, 886–907.

Cengeloglu, Y., Tor, A., Ersoz, M., & Arslan, G. (2006). Removal of nitrate from aqueous solution by using red mud. *Separation and Purification Technology, 51*, 374–378.

Cho, D., Chon, C., Kim, Y., Jeon, B., Schwartz, F. W., Leed, E., & Songe, H. (2011). Adsorption of nitrate and Cr(VI) by cationic polymer-modified granular activated carbon. *Chemical Engineering Journal, 175*, 298–305.

Cochard, R., & Jackes, B. R. (2005). Seed ecology of the invasive tropical tree *Parkinsonia aculeata. Plant Ecology, 180*, 13–31.

CSIRO (Commonwealth Scientific and Industrial Research Organisation) (2011) http://www.csiro.au/en/Outcomes/Food-and-Agriculture/Parkinsonia-biocontrol-agent-seed-feeding-beetle.aspx. Accessed 20 Nov 2014.

Demiral, H., & Gündüzoğlu, G. (2010). Removal of nitrate from aqueous solutions by activated carbon prepared from sugar beet bagasse. *Bioresource Technology, 101*, 1675–1680.

Deveze, M. (2004) Parkinsonia: approaches to the management of Parkinsonia (*Parkinsonia aculeata*) in Australia. The State of Queensland, Department of Natural Resources, Mines and Energy. http://www.weeds.org.au/WoNS/Parkinsonia/docs/Parkinsonia_Mgmnt-1.pdf. Accessed 4 Sept 2014.

Fernandez, M. E., Nunell, G. V., Bonelli, P. R., & Cukierman, A. L. (2012). Batch and dynamic biosorption of basic dyes from binary solutions by alkaline-treated cypress cone chips. *Bioresource Technology, 106*, 55–62.

Fu, P., Hu, S., Xiang, J., Sun, L., Yang, T., Zhang, A., & Zhang, J. (2009). Mechanism study of rice straw pyrolysis by fourier transform infrared technique. *Chinese Journal of Chemical Engineering, 17*, 522–529.

Ganesan, P., Kamaraj, R., & Vasudevan, S. (2013). Application of isotherm, kinetic and thermodynamic models for the adsorption of nitrate ions on graphene from aqueous solution. *Journal of the Taiwan Institute of Chemical Engineers, 44*, 808–814.

Ho, Y. S. (2006). Review of second-order models for adsorption systems. *Journal of Hazardous Materials, 136*, 681–689.

Huidobro, A., Pastor, A. C., & Rodriguez-Reinoso, F. (2001). Preparation of activated carbon cloth from viscous rayon part IV: chemical activation. *Carbon, 39*, 389–398.

Islam, M., & Patel, R. (2010). Synthesis and physicochemical characterization of Zn/Al chloride layered double hydroxide and evaluation of its nitrate removal efficiency. *Desalination, 256*, 120–128.

Ji, B., Wang, H., & Yang, K. (2014). Nitrate and COD removal in an upflow biofilter under an aerobic atmosphere. *Bioresource Technology, 158*, 156–160.

Kante, K., Nieto-Delgado, C., Rangel-Mendezb, J. E., & Bandosz, T. J. (2012). Spent coffee-based activated carbon: specific surface features and their importance for H_2S separation process. *Journal of Hazardous Materials, 201–202*, 141–147.

Keränen, A., Leiviskä, T., Gao, B., Hormi, O., & Tanskanen, J. (2013). Preparation of novel anion exchangers from pine saw dust and bark, spruce bark, birch bark and peat for the removal of nitrate. *Chemical Engineering Science, 98*, 59–68.

Kilpimaa, S., Runtti, H., Kangas, T., Lassi, U., & Kuokkanen, T. (2014). Removal of phosphate and nitrate over a modified carbon residue from biomass gasification. *Chemical Engineering Research and Design, 92*, 1923–1933.

Loganathan, P., Vigneswaran, S., & Kandasamy, J. (2013). Enhanced removal of nitrate from water using surface modification of adsorbents. A review. *Journal of Environmental Management, 131*, 36–374.

Lorenc-Grabowska, E., Gryglewicz, G., & Machnikowski, J. (2010). p-Chlorophenol adsorption on activated carbons with basic surface properties. *Applied Surface Science, 256*, 4480–4487.

Mahmudov, R., & Huang, C. P. (2011). Selective adsorption of oxyanions on activated carbon exemplified by Filtrasorb 400 (F400). *Separation and Purification Technology, 77*, 294–300.

Martín-González, M. A., González-Díaz, O., Susial, P., Araña, J., Herrera-Melián, J. A., Doña-Rodríguez, J. M., & Pérez-Peña, J. (2014). Reuse of Phoenix canariensis palm frond mulch as biosorbent and as precursor of activated carbons for the adsorption of Imazalil in aqueous phase. *Chemical Engineering Journal, 245*, 348–358.

McKay, G., Mesdaghinia, A., Nasseri, S., Hadi, M., & Aminabad, M. S. (2014). Optimum isotherms of dyes sorption by activated carbon: fractional theoretical capacity & error analysis. *Chemical Engineering Journal, 251*, 236–247.

Moussavi, G., Alahabadi, A., Yaghmaeian, K., & Eskandari, M. (2013). Preparation, characterization and adsorption potential of the NH_4Cl-induced activated carbon for the removal of amoxicillin antibiotic from water. *Chemical Engineering Journal, 217*, 119–128.

Mukherjee, R., & De, S. (2014). Adsorptive removal of nitrate from aqueous solution by polyacrylonitrile–alumina nanoparticle mixed matrix hollow-fiber membrane. *Journal of Membrane Science, 466*, 281–292.

Nunell, G.V. (2013) PhD. Thesis, University of Buenos Aires (UBA).

Nunell, G. V., Fernandez, M. E., Bonelli, P. R., & Cukierman, A. L. (2012). Conversion of biomass from an invasive species into activated carbons for removal of nitrate from wastewater. *Biomass and Bioenergy, 44*, 87–95.

Ota, K., Amano, Y., Aikawa, M., & Machida, M. (2013). Removal of nitrate ions from water by activated carbons (ACs)—Influence of surface chemistry of ACs and coexisting chloride and sulfate ions. *Applied Surface Science, 276*, 838–842.

Öztürk, N., & Bektas, T. (2004). Nitrate removal from aqueous solution by adsorption onto various materials. *Journal of Hazardous Materials, 112*, 155–162.

Popescu, M. C., Froidevaux, J., Navi, P., & Popescu, C. M. (2013). Structural modifications of Tilia cordata wood during heat treatment investigated by FT-IR and 2D IR correlation spectroscopy. *Journal of Molecular Structure, 1033*, 176–186.

Sahinkaya, E., Kilic, A., & Duygulu, B. (2014). Pilot and full scale applications of sulfur-based autotrophic denitrification process for nitrate removal from activated sludge process effluent. *Water Research, 60*, 210–217.

Sangwichien, C., Aranovich, G. L., & Donohue, M. D. (2002). Density functional theory predictions of adsorption isotherms with hysteresis loops. *Colloids and Surfaces A: Physicochemical and Engineering Aspects, 206*, 313–320.

Seliem, M. K., Komarneni, S., Byrne, T., Cannon, F. S., Shahien, M. G., Khalil, A. A., & Abd El-Gaid, I. M. (2013). Removal

of nitrate by synthetic organosilicas and organoclay: kinetic and isotherm studies. *Separation and Purification Technology, 110*, 181–187.

Singh, S. K., Townsend, T. G., Mazyck, D., & Boyer, T. H. (2012). Equilibrium and intra-particle diffusion of stabilized landfill leachate onto micro- and meso-porous activated carbon. *Water Research, 46*, 491–499.

Wan, D., Liu, H., Liu, R., Qua, J., Li, S., & Zhang, J. (2012). Adsorption of nitrate and nitrite from aqueous solution onto calcined (Mg–Al) hydrotalcite of different Mg/Al ratio. *Chemical Engineering Journal, 195–196*, 241–247.

Wang, Y., Gao, B., Yue, W., & Yue, Q. (2007). Adsorption kinetics of nitrate from aqueous solutions onto modified wheat residue. *Colloids and Surfaces A: Physicochemical and Engineering Aspects, 308*, 1–5.

Xiao, H., Peng, H., Deng, S., Yang, X., Zhang, Y., & Li, Y. (2014). Preparation of activated carbon from edible fungi residue by microwave assisted K_2CO_3 activation-application in reactive black 5 adsorption from aqueous solution. *Bioresource Technology, 111*, 127–133.